Estimation of Quantum Correlations in Nuclear Spin Ensembles

IISER PUNE

A thesis submitted towards partial fulfilment of
BS-MS Dual Degree Programme

by

HEMANT KATIYAR

under the guidance of

DR. T. S. MAHESH
ASSISTANT PROFESSOR
DEPARTMENT OF PHYSICS
IISER, PUNE

INDIAN INSTITUTE OF SCIENCE EDUCATION AND RESEARCH
PUNE

Certificate

This is to certify that this thesis entitled "Estimation of Quantum Correlations in Nuclear Spin Ensembles" submitted towards the partial fulfilment of the BS-MS dual degree programme at the Indian Institute of Science Education and Research Pune represents original research carried out by "Hemant Katiyar" at "IISER Pune", under the supervision of "Dr. T S Mahesh" during the academic year 2011-2012.

Student
HEMANT KATIYAR

Supervisor
DR. T S MAHESH

Acknowledgements

The most momentous role in fifth year is played by the advisor. Working under Dr. T S Mahesh has been an intriguing and mesmerizing experience. His approach in this fifth year of mine, in providing the complete independence in choosing the problem and the pace at which to solve them, has been a great edification. His deep understanding of the subject, giving the freedom to collaborate and placid nature has been a continuous source of inspiration.

All persons are affected by their surrounding, even more if it offers them what they aspire. Working in the NMR lab has given me an opportunity to work with some really talented and hard-working individuals. I think with their company, i myself is becoming a hard-working person, though i have been told it's hardly noticeable. One important contribution is by Soumya, who I have had chance to work most of the time during the project. I can say that he have been my assistant advisor. Discussing with other members of the group Abhishek, Manvendra and swathi, not necessarily academic stuff, has been fun.

I am also indebted to Dr. Santhanam under which i did my first research project, and for his excellent Quantum Mechanics courses.

The next two teachers I like to acknowledge are not even official teachers: Shadab Alam(a.k.a Duss Guru) and Anuj more. Taking their advice consciously and unconsciously has been always worthwhile. My friends Vibham, Ajinkya , Dinesh, Karan, Sandeep and Prashant has always provided me with an asylum from the academic life. One of the most crucial role, throughout my life in IISER is played by my seniors Ashutosh, Hemant and Smrati, their teaching of the worldly matters is been an unforgettable experience.

Abstract

We study evolution of quantum correlations in ensembles of two-qubit nuclear spin systems via nuclear magnetic resonance techniques. We use discord as a measure of quantum correlations and the Werner state as an explicit example. We first introduce different ways of measuring discord and geometric discord in two-qubit systems, and then we describe (a) quantitative measurement of discord for Werner-like states prepared using an entangling pulse sequence, (b) the efficiency of dynamical decoupling sequences in preserving quantum correlations,(c) the evolution of discord for a singlet-triplet mixed state during a radio-frequency spin-lock, and(d)measuring geometric discord for three-qubit case taking $|S_0\rangle \otimes |0\rangle$ and GHZ state as an example.

List Of Publications

- Estimation of Quantum Correlations in Two-Qubit NMR systems,
  <u>Hemant Katiyar</u>, S S Roy, T S Mahesh and Apoorva Patel,
  <u>*eprint* :</u> arXiv:1203.1756v1, submitted to *Phys. Rev. A*

Contents

Chapter 1

Introduction

From the moment absurdity is recognized, it becomes a passion, the most harrowing of all.

– Albert Camus in The myth of Sisyphus.

Quantum information science is a fascinating field of study, not only from the scientific research, but also from an economic and commercial point of view. It promises quantum algorithms which are far efficient than the best known classical algorithms. The word efficient here does not mean it's regular meaning - 'clock speed'. An algorithm is considered efficient if it uses polynomial amount of resource. To make this statement explicit we should learn about some notations of complexity theory. An algorithm uses some amount of resource to perform certain computational task, the resource may be 'time'(computational time) or 'space'(number of registers). The amount of resource used by an algorithm is characterized as a function of length of the input. Suppose we have an n-bit input and the algorithm is performed in $5n^4 + 3n + 1$ units of time then we say the amount of resource used is in $O(n^4)$, where $O(.)$ stands for upper bound of the resource used. For polynomial algorithm, resource used is in $O(n^m)$ for an integer m, for linear algorithm it is in $O(n)$ and for logarithmic algorithms, in $O(\log n)$. Since linear and logarithmic functions grow slower than polynomial, they are also considered efficient. However if the resource used is in $\Omega(a^n)$(Ω represents the lower bound) for a constant a, then the algorithm is called 'superpolynomial' or 'exponential'. These algorithms grow faster than polynomial and are considered inefficient. One may be wondering about the use of such coarse measurement of the amount of resource used. This is essential to make the

estimate ignorant of the machine used to implement the algorithm. Let us revisit the above example of the algorithm that takes n-bit input and performs the task in $5n^4 + 3n + 1$ units of time. Suppose another computer performs the same task in $4n^4 + n + 1$ units of time. The study of complexity of the algorithm will depend on the machine used to perform it. To avoid this machine dependence we use the upper bound. As a general rule one computer can always simulate other, but the question is how efficiently. Simulating a quantum system consisting of n quantum bits(qubits) on a classical computer will require in general 2^{2n} complex numbers. Hence a system consisting of around 40 qubits will be nearly impossible to simulate. A quantum computer will require only $O(n)$ number of qubits. In 1982, Feynman introduced the idea of building the quantum computer to the perform these computational tasks. As we can notice that the computers are getting smaller as well as faster with the advance in technology. The number of transistors that can be placed on a Integrated circuit is getting doubled every two years. This trend was predicted by Gordon E. Moore in 1965, and is famously known as Moore's law. As the transistors are getting smaller and smaller the quantum limit will be reached eventually. So it is essential to understand the working of quantum mechanics to harness the right power for computing. These two motivations are worthy enough to pursue research in the field of quantum information science.

As of now, it is known that quantum speed-up is not uniform for all computational tasks. There exist quantum algorithms which provide exponential speed-up for certain tasks: for example (i) Shor's algorithm for prime factorization[1] and (ii) Seth Lloyd's algorithm for solving a system of linear equations[2]. For certain other tasks, there exist quantum algorithms which provide polynomial speed-up: example (i) Grover's algorithm for searching in an unsorted database[3] and (ii) Jordan's algorithm for numerical gradient estimation[4]. For certain tasks, such as parity estimation, there is no quantum speed-up.

One important ingredient in these quantum algorithms is entanglement. Since its introduction by Schrödinger, entanglement has remained an extensively studied and yet a mysterious aspect of quantum theory. Entanglement appears as a byproduct of the quantum formalism that assigns probability amplitudes to physical states and lets them exist in coherent superposition. Although, it runs counter to the human intuition gained through experiences with classical systems, experimental evidence has consistently favoured the existence of such superposed quantum states. Entanglement was thought to be an indispensable resource for quantum information processing.

There have been long debates on the necessity of entanglement for quantum information processing. It is known that conventional nuclear magnetic

resonance (NMR) systems have no entanglement [5, 6], but they are still an efficient test-bed for quantum algorithms [7]. Jozsa and Linden [8] showed that for a pure state quantum computation to be exponentially faster that the classical ones the amount of entanglement should not be bounded by the size of the system. Furthermore, Knill and Laflamme proposed an algorithm, called DQC1, which estimates the trace of any unitary matrix faster than any known classical algorithm [9] and have vanishingly small entanglement. These facts suggests that there is a need to look beyond entanglement.

Entanglement is a witness of non-classicality, and entangled systems violate suitable Bell's inequalities that must be satisfied by all classical systems [10]. Separable (i.e. not entangled) states satisfy such inequalities, and hence were considered insufficient to implement quantum information processing. That belief has changed since Ollivier and Zurek [11] as well as Henderson and Vedral [12] independently introduced a new measure of non-classical correlations named 'discord'. Discord is based on the measure of mutual information between two parts of a system. It is equivalent to entanglement when the system is in a pure state, but unlike entanglement it can be nonzero for separable mixed states.

Datta *et al.* showed that entanglement in the DQC1 algorithm is vanishingly small, and it further decays with increase in the number of qubits [13]. They also showed that the DQC1 algorithm involves non-zero discord. Since discord can be used to quantify the non-classicality of all quantum states (separable as well as entangled), it can be considered the right measure to assess the usefulness of a system for quantum information processing. Thus our present notion of quantum speed up is tied to discord rather than entanglement [14]. For a more detailed review on various other aspects and interpretation of discord, one may refer to an interesting review in Ref.[15].

Discord happens to be one of the many quantities that can measure the non-classicality of a given quantum system. Its standard definition equates discord to the difference between two classically equivalent forms of mutual information. Due to the difficulty in measuring this difference, Dakic *et al.* proposed an alternate quantity called 'geometric discord'. It is the distance between the given quantum state and the closest classical state, and is easier to quantify than discord [16]. We look at both of these quantities in our study.

Several experiments to demonstrate quantum correlations in liquid state NMR systems have been performed in recent years, e.g. by measuring a suitable witness operator [17], by measuring discord [18], and by evaluating the Leggett-Garg inequality [19]. Measurements of discord in mixed states have also been performed using optical systems [20], and quadrupolar NMR systems [21]. Here we report an experimental study of time evolution of

discord in NMR systems. After preparing a two-qubit Werner state, we study the accumulation of discord, effects of dynamical decoupling sequences on it, and its decay due to decoherence. In chapter 2, we revisit some theoretical aspects of discord, and describe different ways of measuring it for the Werner state. Then in chapter 3, we present the experimental details and discuss the results. We conclude in chapter 4 with some inferences from our analysis.

Chapter 2

Theory

2.1   Background

You can't just turn on creativity like a faucet. You have to be in the right mood.
What mood is that?
Last-minute panic.

– Bill Watterson in Calvin and Hobbes.

For the realization of quantum computation and communication Divincenzo has put forward 5 requirements known as the the Divincenzo's criteria[22]

- A scalable physical system with well characterized qubits.

- The ability to initialize the state of the qubits to a simple ïňĄducial state, such as $|000\cdots\rangle$.

- Long relevant decoherence times, much longer than the gate operation time.

- A universal set of quantum gate.

- A qubit-specific measurement capability.

A quantum machine that satisfies all these criteria is still far from inception. But there are systems which can simulate some properties of quantum computer without satisfying all the criterias. The best example is liquid NMR systems. They do not have an initial pure state but a pseudo-pure state

with which we can imitate the working of a pure state. Due to highly mixed nature of states present in NMR they exhibit no entanglement at room temperature. Also NMR systems suffer from an exponential loss of signal with increase in the number of qubits, which asserts the point that NMR systems are not scalable and the ultimate quantum computer might not be the one made of NMR. Our focus is on the 2nd criteria, which states that we should have a pure state to initialize our quantum algorithms. The question is that when working with the mixed states, is entanglement necessary? The answer seems to be no, the main reason is one behind the working of DQC1 algorithm proposed by Knill and Laflamme[9] to calculate the trace of any unitary matrix. This algorithm provides an exponential speed up over best known classical algorithm and possesses vanishingly small entanglement[13]. Another reason to support the non-necessity of entanglement is that there are various quantum cryptography protocols do not require entanglement [23].

Now the question arises that if entanglement is not a necessary condition then what it is that is giving the exponential speed up to DQC1 and quantum algorithm performed in liquid state NMR experiment at room temperature. They answer may be another type of quantum correlation quantified by discord that is present even in separable states. It has been shown by Animesh et al that DQC1 possesses a non-zero amount of discord[13]. Here in this thesis we try to measure the amount of discord present in a two qubit NMR systems by using werner states as an explicit example. Then we measure the efficiency of various dynamical decoupling sequences in preserving discord and finally the evolution of discord for a singlet triplet mixed state during a radio-frequency spin-lock. Then we define the scheme of measuring geometric discord in case of 3 qubits. The aim of this chapter is to provide a theoretical background.

2.2   Quantum Discord

Conditional Entropy:

In classical information theory the amount of information contained in a random variable X is quantified as the Shannon entropy,

$$H(X) = -\sum_x p_x \log_2 p_x \ , \tag{2.1}$$

where p_x is the probability of occurrence of event X. When $H(X) = 0$, the random variable X is completely determined and no new information is gained by measuring it. Hence, Shannon entropy can be interpreted as either

the uncertainty before measuring a random variable or the information gained upon measuring it. To see a mathematical proof of why Shannon entropy represents information content reader is encouraged to refer to appendix A of Ref[24]

Consider a bipartite system containing two subsystems (or random variables), A and B. Conditional entropy of B quantifies the uncertainty in measurement of B when A is known, and is represented by $H(B|A)$. Using classical probability theory, it can be expressed as

$$H(B|A) = H(A, B) - H(A) \ , \tag{2.2}$$

where $H(A, B)$ is the information content of the full system and $H(A)$ is the information content of the subsystem A. An equivalent way of defining the conditional entropy is

$$H(B|A) = \sum_i p_i^a H(B|a = i) \ , \tag{2.3}$$

where

$$H(B|a = i) = -\sum_j p(b_j|a_i) \log_2 p(b_j|a_i) \ , \tag{2.4}$$

and $p(b_j|a_i)$ is the conditional probability of occurrence of event b_j given that event a_i has occurred. Unlike the definition in Eq.(2.2), the definition in Eq.(2.3) involves measurement of one subsystem of a bipartite system.

Mutual Information:

It is the amount of information that is common to both the subsystems of a bipartite system, and is given by

$$I(A : B) = H(A) + H(B) - H(A, B) \ . \tag{2.5}$$

This expression can be intuitively understood with the help of Fig. 2.1. On the right hand side, the first two terms quantify the information content of subsystems A and B respectively. So the information common to both the subsystems is counted twice. Subtracting the information content of the combined system then gives the common (or mutual) information. The result is clearly symmetric, i.e. $I(A : B) = I(B : A)$. A classically equivalent form of mutual information, also visible in Fig. 2.1, is

$$\begin{aligned} J(A : B) &= H(B) - H(B|A) \\ &= H(B) - \sum_i p_i^a H(B|a = i) \ , \end{aligned} \tag{2.6}$$

which removes from the information content of subsystem B the conditional contribution that is not contained in subsystem A.
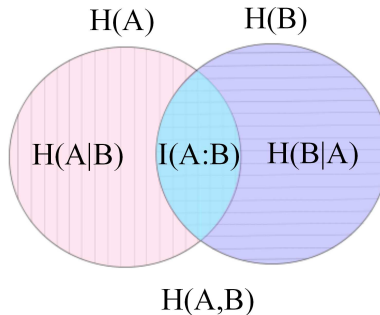

Figure 2.1: The Venn diagram representing total information $H(A, B)$, individual informations ($H(A)$, $H(B)$), conditional information ($H(A|B)$, $H(B|A)$), and mutual information $I(A : B) = J(A : B)$ in classical information theory.

In quantum information theory, the von Neumann entropy gives the information content of a density matrix,

$$H(\rho) = -\sum_x \lambda_x \log_2 \lambda_x \ , \tag{2.7}$$

where λ_x are the eigenvalues of the density matrix ρ. Although the two expressions of mutual information, Eqs.(2.5) and (2.6), are equivalent in classical information theory, they are not so in quantum information theory. The reason for the difference is that the expression for mutual information given by Eq.(2.5) involves measurement and depends on its outcomes. Measurements in quantum theory are basis dependent and also change the state of the system. Henderson and Vedral [12] have proved that the total classical correlation can be obtained as the largest value of $J(A : B)$, where the maximization is performed over all possible orthonormal measurement bases $\{\Pi_i^a\}$ for A, satisfying $\sum_i \Pi_i^a = \mathbb{1}$ and $\Pi_i^a \Pi_j^a = \delta_{ij} \Pi_i^a$. Therefore, the non-classical correlations can be quantified as the difference

$$D(B|A) = I(A : B) - \max_{\{\Pi_i^a\}} J(A : B) \ . \tag{2.8}$$

Olivier and Zurek named this difference 'discord' [11]. Zero discord states or 'classical' states are the states in which the maximal information about a

9

subsystem can be obtained without disturbing its correlations with the rest of the system.

Discord is not a symmetric function in general, i.e. $D(B|A)$ and $D(A|B)$ can be different. Datta [25] has proved that a state ρ_{AB} satisfies $D(B|A) = 0$ if and only if there exists a complete set of orthonormal measurement operators on A such that

$$\rho_{AB} = \sum_i p_i^a \Pi_i^a \otimes \rho_{B|a=i} \ . \tag{2.9}$$

When one part of a general bipartite system is measured, the resulting density matrix is of the form given by Eq.(2.9). Since the state rendered upon measurement is a classical state, one can extract classical correlations from it. Thus for any quantum state and every orthonormal measurement basis, there exists a classically correlated state. Maximization of $J(A:B)$ captures the maximum classical correlation that can be extracted from the system, and whatever extra correlation that may remain is the quantum correlation.

Quantum states can be correlated in ways that are inaccessible to classical states. For example in the following state, four non-orthonormal states of the first system are correlated with four non-orthonormal states of the second system [16]:

$$\rho = \frac{1}{4}(|+\rangle\langle+| \otimes |0\rangle\langle0| + |-\rangle\langle-| \otimes |1\rangle\langle1|$$
$$+|0\rangle\langle0| \otimes |-\rangle\langle-| + |1\rangle\langle1| \otimes |+\rangle\langle+|) \ . \tag{2.10}$$

The discord for this state is 0.3113.

To see that discord is non-zero even for separable mixed states, let us take the example of Werner state, $\rho_W(\epsilon) = \frac{1-\epsilon}{4}\mathbb{1} + \epsilon|\psi^-\rangle\langle\psi^-|$ where $|\psi^-\rangle = \frac{1}{\sqrt{2}}(|01\rangle - |10\rangle)$, and plot discord and entanglement in fig2.2.we can clearly see that the entanglement goes to zero when $\epsilon \leq \frac{1}{3}$, which means the state is separable in this range, but discord posses non-zero value.
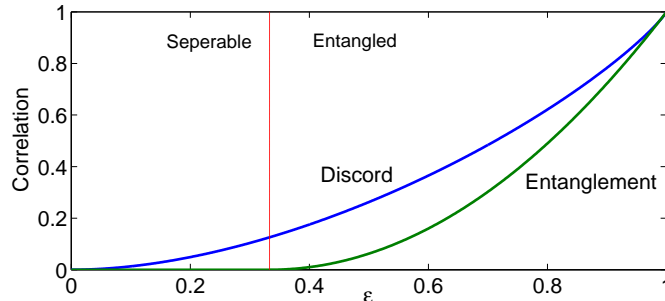

Figure 2.2: Discod and Entanglement values for the werner state

2.3 Evaluation of Discord

Given a density matrix ρ_{AB}, it is easy to construct the reduced density matrices ρ_A and ρ_B, and then obtain the total correlation $I(A : B)$ using Eq.(2.5). Maximization of $J(A : B)$ to evaluate discord is non-trivial, however. The brute force method is to maximize $J(A : B)$ over as many orthonormal measurement bases as possible, taking into account all constraints and symmetries. For a general quantum state, a closed analytic formula for discord does not exist, but for certain special class of states analytical results are available [26]. For example, Chen *et al.* have described analytical evaluation of discord for two qubit X-states under specific circumstances [27]. Luo has given an analytical formula for discord of the Bell-diagonal states that form a subset of X-states [28]. In our work, we have evaluated discord using both the brute force method and the Luo method.

Extensive measurement method: This method involves measurements over extensive sets of orthonormal basis vectors and maximization of $J(A : B)$. For measurement of a single qubit in a two qubit system, we use the orthonormal basis

$$\{|u\rangle = \cos\theta|0\rangle + e^{i\phi}\sin\theta|1\rangle \ , \ |v\rangle = \sin\theta|0\rangle - e^{i\phi}\cos\theta|1\rangle\} \ , \qquad (2.11)$$

and let $\cos\theta \in [-1, 1]$ and $\phi \in [0, 2\pi)$ vary in small steps. For every choice of θ and ϕ, we project the experimental density matrix obtained by tomography along the orthonormal basis. The post-projection density matrix is

$$\rho' = \sum_{i=u,v} \Pi_i^a \rho \Pi_i^a = \sum_{i=u,v} p_i^a \Pi_i^a \otimes \rho_{B|a=i} \ , \qquad (2.12)$$

with $p_i^a = \text{Tr}[\Pi_i^a \rho]$. Discord is then obtained from the conditional density matrix $\rho_{B|a=i}$ as per Eqs.(2.6,2.8).

Strictly speaking, this method gives a lower bound on $J(A : B)$, since the direction maximizing $J(A : B)$ may not exactly match any of the points on the discrete (θ, ϕ) grid. Also, when the desired state is isotropic, e.g. the Werner state, the angular variation of $J(A : B)$ provides an estimate of the inaccuracy in the state preparation, e.g. due to inhomogeneities and pulse imperfections.

Analytical method for the Bell-diagonal states: As the name suggests, the Bell-diagonal states are diagonal in the Bell basis, given by

$$|\psi^\pm\rangle = \frac{1}{\sqrt{2}}(|01\rangle \pm |10\rangle) \ , \ \ |\phi^\pm\rangle = \frac{1}{\sqrt{2}}(|00\rangle \pm |11\rangle) \ . \qquad (2.13)$$

The generic structure of a Bell-diagonal state is $\rho_{BD} = c_1|\psi^-\rangle\langle\psi^-| + c_2|\psi^+\rangle\langle\psi^+| + c_3|\phi^-\rangle\langle\phi^-| + c_4|\phi^+\rangle\langle\phi^+|$. With only local unitary operations (so as not to

alter the correlations), all Bell-diagonal states can be transformed to the form

$$\rho_{BD} = \frac{1}{4}\left(\mathbb{1} + \sum_{j=1}^{3} r_j \sigma_j \otimes \sigma_j\right), \tag{2.14}$$

where the real numbers r_j are constrained so that all eigenvalues of ρ_{BD} remain in $[0, 1]$. The symmetric form of ρ_{BD} also implies that it has symmetric discord, i.e. $D_{BD}(B|A) = D_{BD}(A|B)$.

Luo choose the set of measurement basis as $\{V\Pi_k^a V^\dagger\}$, where $\Pi_k^a = |k\rangle\langle k|$ are the projection operators for the standard basis states $(k = 0, 1)$, and V is an arbitrary $SU(2)$ rotation matrix. A projective measurement yields the probabilities $p_0 = p_1 = \frac{1}{2}$, and an analytical formula for the classical correlation,

$$\max_{\{\Pi_k^a\}} J(A : B) = \left(\frac{1-r}{2}\right)\log_2(1-r) + \left(\frac{1+r}{2}\right)\log_2(1+r), \tag{2.15}$$

with $r = \max\{|r_1|, |r_2|, |r_3|\}$.

For the Bell-diagonal states, the reduced density matrices are $\rho_A = \rho_B = \mathbb{1}/2$, and the total correlation becomes

$$I(A : B) = 2 + \sum_{i=1}^{4} \lambda_i \log_2 \lambda_i, \tag{2.16}$$

where the eigenvalues λ_i of ρ_{BD} are:

$$
\begin{aligned}
\lambda_1 &= (1 - r_1 - r_2 - r_3)/4 \\
\lambda_2 &= (1 - r_1 + r_2 + r_3)/4 \\
\lambda_3 &= (1 + r_1 - r_2 + r_3)/4 \\
\lambda_4 &= (1 + r_1 + r_2 - r_3)/4.
\end{aligned} \tag{2.17}
$$

Thus the analytical formula for discord is, as per Eq.(2.8),

$$
\begin{aligned}
D_{BD}(B|A) = {}& 2 + \sum_{i=1}^{4} \lambda_i \log_2 \lambda_i - \left(\frac{1-r}{2}\right)\log_2(1-r) \\
& - \left(\frac{1+r}{2}\right)\log_2(1+r).
\end{aligned} \tag{2.18}
$$

For a Werner state of the form,

$$\rho_W(\epsilon) = \frac{1-\epsilon}{4}\mathbb{1} + \epsilon|\psi^-\rangle\langle\psi^-|, \tag{2.19}$$

12

$r_j = -\epsilon$ and $r = \epsilon$. The discord is then given by

$$
\begin{aligned}
D_W(\epsilon) &= \frac{1}{4}\log_2\frac{(1-\epsilon)(1+3\epsilon)}{(1+\epsilon)^2} \\
&+ \frac{\epsilon}{4}\log_2\frac{(1+3\epsilon)^3}{(1-\epsilon)(1+\epsilon)^2} \\
&= \frac{\epsilon^2}{\ln 2} + O(\epsilon^3) \; .
\end{aligned}
\tag{2.20}
$$

This expression is plotted versus the purity ϵ in Fig. 2.3, together with the corresponding correlations $I(A:B)$ and $J(A:B)$.

In practice, the experimental density matrix obtained by tomography is not necessarily Bell-diagonal. We obtain $I(A:B)$ as before, using Eq.(2.5). To extract the maximum value of $J(A:B)$, we drop the the off-diagonal terms, keeping only the terms in Eq.(2.14), and use Eq.(2.15). In this procedure, discord is overestimated, whenever the actual direction maximizing $J(A:B)$ is not in the Bell-diagonal state subspace.

2.4 Geometric Discord

Since the maximization of $J(A:B)$ involved in calculating discord is a hard problem, Dakic *et al.* introduced a more easily computable form of discord based on a geometric measure [16]. For every quantum quantum state there is a set of post-measurement classical states, and the geometric discord is defined as the distance between the quantum state and the nearest classical state,

$$
DG(B|A) = \min_{\chi \in \Omega_0} \|\rho - \chi\|^2 \; ,
\tag{2.21}
$$

where Ω_0 represents the set of classical states, and $\|X - Y\|^2 = \mathrm{Tr}(X-Y)^2$ is the Hilbert-Schmidt quadratic norm. Obviously, $DG(B|A)$ is invariant under local unitary transformations. Analytical formula for computing geometric discord for an arbitrary $A_{m\times m} \otimes B_{n\times n}$ state of a bipartite quantum system is available [29]. Recently discovered ways to calculate lower bounds on discord for such general states do not require tomography, and hence are friendlier experimentally [30, 31]. We follow the formalism of Dakic *et al.* [16] to obtain geometric discord for two-qubit states. The two-qubit density matrix in the Bloch representation is

$$
\rho = \frac{1}{4}\Big(\mathbb{1}\otimes\mathbb{1} + \sum_{i=1}^{3} x_i\sigma_i\otimes\mathbb{1} + \sum_{i=1}^{3} y_i\mathbb{1}\otimes\sigma_i + \sum_{i,j=1}^{3} T_{ij}\sigma_i\otimes\sigma_j\Big)
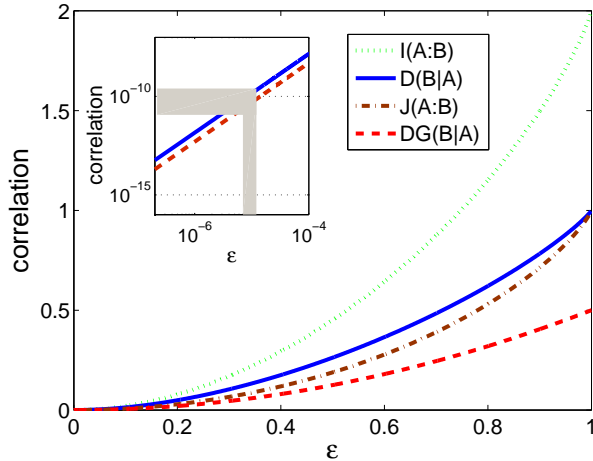\tag{2.22}
$$

Figure 2.3: Various correlations as functions of the purity ϵ, for Werner states of the form given in Eq.(2.19). The inset shows the range of discord for the purity available in our NMR setup.

where x_i and y_i represent the Bloch vectors for the two qubits, and $T_{ij} = \text{Tr}(\rho(\sigma_i \otimes \sigma_j))$ are the components of the correlation matrix, T. The geometric discord for such a state is

$$DG(B|A) = \frac{1}{4}(\|x\|^2 + \|T\|^2 - \eta_{\max}) \ , \qquad (2.23)$$

where $\|T\|^2 = \text{Tr}[T^T T]$, and $\eta_{\max}$ is the largest eigenvalue of $\vec{x}\vec{x}^T + TT^T$.

For the Werner state, as already mentioned, $x_i = 0 = y_i$ and T is a diagonal matrix with $T_{ii} = -\epsilon$. Then $\|T\|^2 = 3\epsilon^2$ and all eigenvalues of TT^T are ϵ^2, yielding

$$DG_W(\epsilon) = \frac{1}{4}(3\epsilon^2 - \epsilon^2) = \frac{\epsilon^2}{2}. \qquad (2.24)$$

This expression is also plotted versus the purity ϵ in Fig. 2.3. Comparison with Eq.(2.20) reveals that discord and geometric discord are proportional for low purity Werner states. Also, the numerical difference between $D_W(\epsilon)$ and $2DG_W(\epsilon)$ does not exceed 0.027 for all $\epsilon \in [0, 1]$.

The Bloch parameters x_i, y_i and T_{ij} provide a complete description of any two-qubit state. So tomographic measurement of these parameters determines the geometric discord exactly by Eq.(2.23).

2.4.1 Geomtric Discord in case of 3 qubits

Hassan and Joag provided an analytical formula for calculation of geometric discord for a n-qubit state[32]. In this thesis we will provide the same formula but for 3-qubit case.

Let N be a set such that $N = \{k_i : i = 1, 2, 3\}$, where k_i denotes the 3 qubits. The variables $\alpha_{k_i} = 1, 2, 3$, spans the Pauli operators ($\{\sigma_1, \sigma_2, \sigma_3\}$) for the k_i^{th} qubit, and

$$
\begin{aligned}
\sigma_{\alpha_{k_1}}^{(k_1)} &= (\sigma_{\alpha_{k_1}} \otimes I \otimes I), \\
\sigma_{\alpha_{k_1}}^{(k_1)} \sigma_{\alpha_{k_2}}^{(k_2)} &= (\sigma_{\alpha_{k_1}} \otimes \sigma_{\alpha_{k_2}} \otimes I),
\end{aligned}
\tag{2.25}
$$

etc. Then the 3-qubit density matrix can be written as

$$
\rho_{123} = \frac{1}{2^3} (\otimes_m^3 I_{d_m} + \sum_{k_1 \in N} \sum_{\alpha_{k_1}} s_{\alpha_{k_1}} \sigma_{\alpha_{k_1}}^{(k_1)} + \sum_{\{k_1, k_2\}} \sum_{\alpha_{k_1}, \alpha_{k_2}} t_{\alpha_{k_1} \alpha_{k_2}} \sigma_{\alpha_{k_1}}^{(k_1)} \sigma_{\alpha_{k_2}}^{(k_2)}
$$
$$
+ \sum_{\alpha_{k_1} \alpha_{k_2} \alpha_{k_3}} t_{\alpha_{k_1} \alpha_{k_2} \alpha_{k_2}} \sigma_{\alpha_1}^{(1)} \sigma_{\alpha_2}^{(2)} \sigma_{\alpha_3}^{(3)}) \tag{2.26}
$$

where $s(k_i)$ is the bloch vector for k_i^{th} qubit. Let $T^{\{k_1, \cdots, k_M\}} = [t_{\alpha_{k_1} \cdots \alpha_{k_M}}]$, which are defined by

$$
t_{\alpha_{k_1} \cdots \alpha_{k_M}} = tr[\rho_{123} \sigma_{\alpha_{k_1}}^{(k_1)} \cdots \sigma_{\alpha_{k_M}}^{(k_M)}]. \tag{2.27}
$$

Then the Geometric discord, if we measure the qubit k is given by,

$$
DG_k(\rho_{123}) = \frac{1}{2^n} \left[\|\vec{s}^{(k)}\|^2 + \sum_{1 \le M \le 2} \sum_{\{k_1, \cdots, k_M\} \in N-k} \|T^{\{k_1, \cdots, k_M, k\}}\|^2 - \zeta_{max} \right].
\tag{2.28}
$$

Here ζ_{max} is the largest eigenvalue of a 3×3 real symmetric matrix $G^{(k)}$, defined as

$$
G^{(k)} = \vec{s}^{(k)} (\vec{s}^{(k)})^t + \sum_{k_1 \in N-k} (T^{\{k_1, k\}})^t T^{\{k_1, k\}} + \mathbb{T}, \tag{2.29}
$$

where $\mathbb{T} = [\tau_{\alpha_k \beta_k}]$ is a 3×3 real matrix defined element wise as

$$
\tau_{\alpha_k \beta_k} = \sum_{\{k_1, k_2\} \in N-k} \sum_{\alpha_{k_1} \alpha_{k_2}} t_{\alpha_{k_1} \alpha_{k_2} \alpha_k} t_{\alpha_{k_1} \alpha_{k_2} \beta_k}
$$

$$
\alpha_{k_i}, \alpha_k, \beta_k = 1, 2, 3; i = 1, 2, 3.
$$

The fig2.4 shows the variation of the geometric discord of the state given by $\rho(\epsilon) = \frac{1-\epsilon}{8} \mathbb{1} + \epsilon |GHZ\rangle\langle GHZ|$, where $|GHZ\rangle = \frac{1}{\sqrt{2}} (|000\rangle + |111\rangle)$.
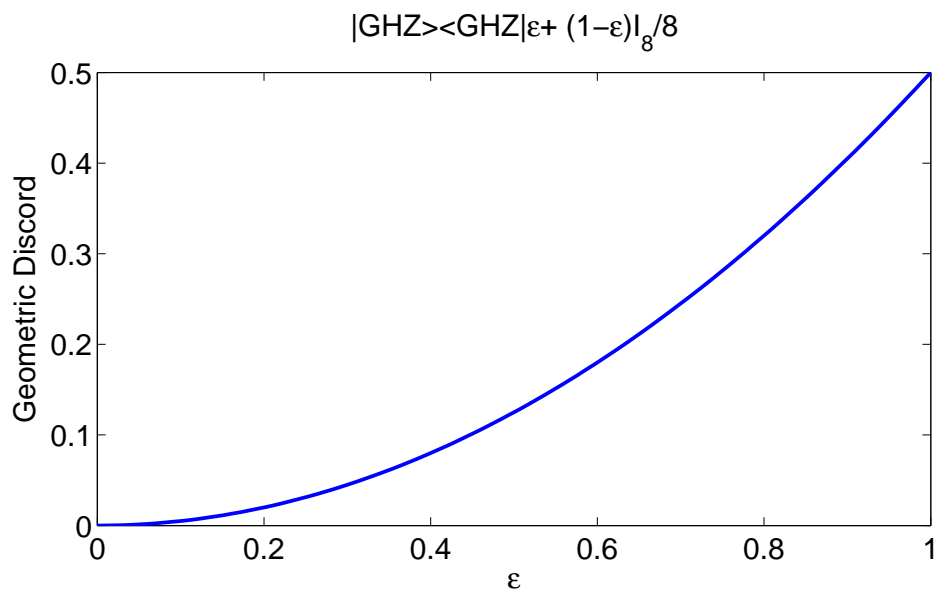
Figure 2.4: Geometric discord for a mixed GHZ state

Chapter 3

Experiments and Results

Discord could be like sunlight, which is plentiful but has to be harnessed in a certain way to be useful. We need to identify what that way is.

– Kavan Modi.[33]

Now we describe experimental evaluation of discord for two-qubit NMR systems. We measured quantum correlations for three different samples, each forming a two-qubit system, under different circumstances.

Sample 1: ^{1}H and ^{13}C spins of ^{13}C-chloroform (see Fig. 3.1a) dissolved in deuterated chloroform ($CDCl_3$). Both ^{1}H and ^{13}C spins were on-resonant and the scalar coupling (J) between the two spins is 219 Hz. For the proton, the T1 and T2 relaxation time constants are 14.5 s and 5.7 s respectively. For carbon, they are 21 s and 0.25 s respectively.

Sample 2: ^{1}H nuclear pairs of 5-chlorothiophene-2-carbonitrile (see Fig. 3.4b) dissolved in deuterated dymethylsulfoxside (DMSO-D_6). The chemical shift difference ($\Delta\nu$) and scalar coupling (J) between the two spins are 270 Hz and 4.11 Hz respectively. For each proton, the T1 and T2 relaxation time constants are about 6.3 s and 2.3 s respectively.

To evaluate the quantum correlations in three-qubit systems, we used the third sample.

Sample 3: ^{19}F nuclear spins of trifloroiodoethylene (see Fig. 3.6a) dissolved in acetone-d6. The chemical shifts ($\Delta\nu$) and scalar couplings (J) between the spins are shown in Fig. 3.6b.

All the experiments were carried out in a Bruker 500 MHz NMR spectrometer at an ambient temperature of 300 K. Precise radio-frequency (RF)

gates for the experiments were synthesized by numerical optimizations as described in [34, 35].

3.1 Deviation Density Matrix

In thermal equilibrium at room temperature, kT is much larger than the Zeeman energy splittings. So the density matrix of a two-qubit system can be expanded as

$$\rho_{\text{eq}} = \frac{1}{4} e^{-\mathcal{H}_Z/kT} \approx \frac{1}{4}(\mathbb{1} + \overline{\rho}_{\text{eq}}) \ . \tag{3.1}$$

Here $\mathcal{H}_Z = -\hbar\omega_A(I_z^A + \frac{\omega_B}{\omega_A}I_z^B)$, is the Zeeman Hamiltonian, characterized by the Larmor frequencies ω_A and ω_B and the $z-$components of spin operators I^A and I^B. The identity $\mathbb{1}$ represents a background of uniformly populated levels, and the traceless part $\overline{\rho}_{\text{eq}} = \xi(I_z^A + \frac{\omega_B}{\omega_A}I_z^B)$ is known as the deviation density matrix. Only the traceless part $\overline{\rho}$ is manipulated by unitary transformations in all NMR experiments. For protons in currently available magnetic fields at room temperatures, the small dimensionless number $\xi = \hbar\omega_A/kT \approx 8 \times 10^{-5}$. The discord for this size of purity is shown in the inset of Fig. 2.3 by a shaded area.

3.2 Preparation of Discord

The pulse sequence in Fig. 3.1 was used to prepare discord between ^{1}H and ^{13}C spins of ^{13}C-chloroform. For this system, $\omega_C/\omega_H \approx 1/4$. An initial $|00\rangle$ pseudopure state is prepared using the spatial averaging method [36], as shown in the first part of Fig. 3.1(b). The transformations of the traceless $\overline{\rho}_{\text{eq}}/\xi$ under the spatial averaging pulse sequence are:

$$I_z^A + \tfrac{1}{4}I_z^B$$
$$\downarrow 15_x^{\circ A}$$
$$I_z^A \cos(15^\circ) - I_y^A \sin(15^\circ) + \tfrac{1}{4}I_z^B$$
$$\downarrow \tfrac{1}{2J}$$
$$I_z^A \cos(15^\circ) + 2I_x^A I_z^B \sin(15^\circ) + \tfrac{1}{4}I_z^B$$
$$\downarrow 75_{-y}^{\circ A}, G_z$$
$$I_z^A \cos 15^\circ \cos 75^\circ + 2I_z^A I_z^B \sin 15^\circ \sin 75^\circ + \tfrac{1}{4}I_z^B$$
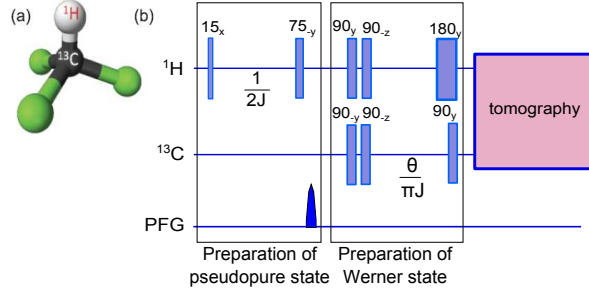$$= \tfrac{1}{4}(I_z^A + I_z^B + 2I_z^A I_z^B). \tag{3.2}$$

Figure 3.1: (a) The molecular structure of ^{13}C-chloroform, and (b) the pulse sequence for discord preparation. In (b), PFG is the pulse field gradient operation which destroys the coherences and retains the diagonal elements of the density matrix.

This pseudopure state is converted into a Werner state, using the second part of the pulse sequence in Fig. 3.1(b) with the delay $\theta/(\pi J) = 1/(2J)$:

$$
\begin{aligned}
\rho_{pp} &= \frac{1}{4}\left[\mathbb{1} + \frac{\xi}{4}\left(I_z^A + I_z^B + 2I_z^A I_z^B\right)\right] \\
&\downarrow \quad \text{Werner pulse sequence} \\
\rho_W &= \frac{1}{4}\left[\mathbb{1} + \frac{\xi}{4}\left(-\frac{1}{2}\mathbb{1} + 2|\psi^-\rangle\langle\psi^-|\right)\right] \\
&= \frac{1-(\xi/8)}{4}\mathbb{1} + \frac{\xi}{8}|\psi^-\rangle\langle\psi^-| \quad (3.3)
\end{aligned}
$$

Comparing with Eq.(2.19), we can see that the relevant purity parameter in this case is $\epsilon = \xi/8$.

3.2.1 Results

We varied θ from 0 to 2π in 13 steps, and for each delay carried out tomography to measure the experimental density matrix [37]. The corresponding simulated density matrices are obtained by assuming perfect pulses and carrying out a calculation similar to Eq.(3.3). It can be easily seen that for θ values that are odd multiples of $\pi/2$, one obtains Bell-diagonal states. We define the fidelity F of a test density matrix ρ_{test} relative to the Werner state as

$$
F = \frac{\text{Tr}[\overline{\rho}_{\text{test}} \cdot \overline{\rho}_W]}{\sqrt{\text{Tr}[\overline{\rho}_{\text{test}}^2]\ \text{Tr}[\overline{\rho}_W^2]}} \ . \quad (3.4)
$$

Fidelities of the experimental and the simulated density matrices, as functions of θ, are shown in Fig. 3.2(a). The discord for each value of θ is obtained
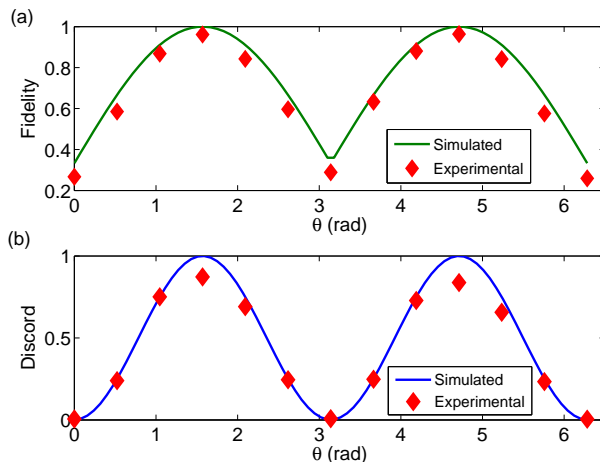
Figure 3.2: (a) Fidelity relative to the Werner state of the experimental and the simulated states as a function of θ, and (b) corresponding discord values in units of $\epsilon^2/\ln 2$. The maximum discord is obtained for the delay parameter $\theta = (2n+1)\pi/2$, corresponding to preparation of Bell-diagonal states.

using the extensive measurement method as described in Section II.B. Both experimental and simulated values of the discord are plotted in Fig. 3.2(b), in units of $\epsilon^2/\ln 2$. The state at $\theta = 0$ is related to the pseudopure $|00\rangle$ state by local unitary transformations, and therefore has zero discord. Otherwise, for $\theta \neq 0$, non-local spin-spin interactions give rise to discord. For θ equal to odd multiples of $\pi/2$, one obtains Bell-diagonal states with maximum discord. For θ equal to π, the delay equals the period of the scalar coupling, implying no transformation, and the discord is periodic thereafter.

3.3 Discord under Dynamical Decoupling

Dynamical decoupling (DD) is a method of preserving coherences in NMR, by frequent modulation of system-bath couplings with the help of a series of π-pulses [38, 39, 40, 41]. We applied DD sequences immediately after obtaining the Werner state as in Eq.(3.3), and followed that up with tomography. The CPMG DD involved a series of uniformly spaced π-pulses separated by 4 ms delays. For comparison, we label as no-DD the evolution with the delays but without the pulses. The Uhrig DD (UDD) involved cycles of a 7-pulse sequence [41, 42]. The time-instant t_j of the jth π-pulse in each cycle was chosen according to Uhrig's formula $t_j = 28 \sin^2(\pi j/16)$ ms [41].
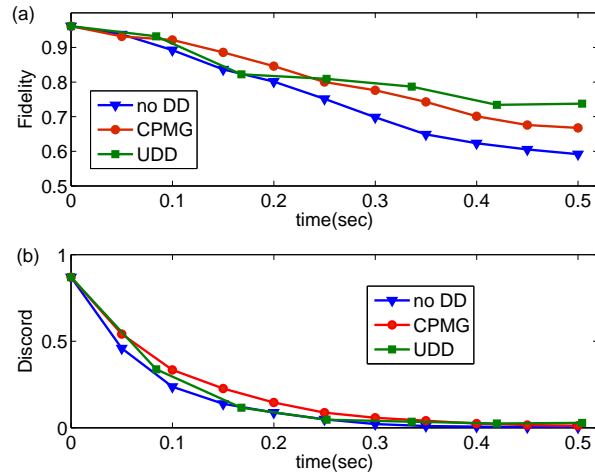
Figure 3.3: (a) Fidelity of the experimental state relative to the Werner state for various DD schemes, and (b) corresponding discord values in units of $\epsilon^2/\ln 2$.

3.3.1 Results

Fig. 3.3(a) shows the time dependence of fidelities relative to the Werner state for no-DD, CPMG DD sequence, and UDD sequence. Fig. 3.3(b) displays the corresponding discord values obtained using the extensive measurement method. We observe that the DD sequences help in protecting fidelities of two-qubit quantum states, in agreement with an earlier work [42]. On the other hand, there is not much difference between no-DD and DD schemes in preserving discord. We believe that the reason is the decay of purity during the DD sequences. While fidelity is measured relative to a particular target state, discord is independent of any target state. Our experiments indicate that though the DD sequences help prevent the quantum state from evolving to other quantum states, they are not useful in keeping the purity from decaying.

3.4   Discord in Long-lived Singlet States

Here we considered a pair of nuclear spins of the same isotope, i.e. *Sample 2* shown in Fig. 3.4(b). The pulse sequence for the preparation of a long-lived singlet state is shown in Fig. 3.4(a). The spin-lock was realized by a low-amplitude continuous RF wave (nutation frequency of 2 kHz). The carrier frequency of the spin-lock was set to $(\omega_A + \omega_B)/2$, the mean Larmor

frequency of the two spins. The average Hamiltonian in the interaction frame during the spin-lock interval is $H_{\text{int}} = 2\pi\hbar J(I_1 \cdot I_2)$, where I_1 and I_2 are the spin operators. The singlet state, and the degenerate triplet states, form an orthonormal eigenbasis of this H_{int}:

$$|S_0\rangle = \frac{1}{\sqrt{2}}(|01\rangle - |10\rangle), \tag{3.5}$$

$$|T_1\rangle = |00\rangle, \ |T_0\rangle = \frac{1}{\sqrt{2}}(|01\rangle + |10\rangle), \ |T_{-1}\rangle = |11\rangle. \tag{3.6}$$

As described earlier, the NMR system under ordinary conditions exists in a highly mixed state with a small purity. Leaving out the uniform distribution, the ground state is the Werner state, which is also called the long-lived singlet state (LLS) [43, 44]. LLS is anti-symmetric with respect to spin-exchange, and is not connected to other eigenstates (i.e. symmetric triplet states) by any symmetry preserving transformations such as the non-selective RF pulses and the intra-pair dipolar interaction. Therefore, LLS can survive for durations much longer than other non-equilibrium spin states. LLS have been used in NMR experiments for the study of slow diffusion [45], for ultra-precise measurement of scalar interactions [46], for storage and transport of parahydrogen [47, 48], and for preparation of high fidelity Bell states and other pseudopure states [49].

The RF pulses prior to the spin-lock prepare a state which is a mixture of the $|S_0\rangle$ and $|T_0\rangle$ states,

$$\rho(0) = \frac{1}{4}\mathbb{1} + \frac{\xi}{4}(|S_0\rangle\langle S_0| - |T_0\rangle\langle T_0|) . \tag{3.7}$$

During the spin-lock, RF pulses mix various components of states with the same spin, and the $|T_0\rangle$ state rapidly equilibrates with the other triplet states. Furthermore, all other coherences created due to pulse imperfections also decay towards the background [50]. Upon this equilibration, which takes a few seconds, the system reaches the Werner state,

$$\rho_{\text{LLS}} = \frac{1 - (\xi/3)}{4}\mathbb{1} + \frac{\xi}{3}|S_0\rangle\langle S_0| = \rho_W(\epsilon = \xi/3). \tag{3.8}$$

This Werner state has a different purity than the one prepared from *Sample 1*, i.e. Eq.(3.3).

To study the evolution of the density matrix state during spin-lock, we applied the spin-lock for a variable duration τ, and then carried out tomography to measure the traceless part of the density matrix $\rho(\tau)$. We find that $\rho(\tau)$ gradually evolves towards the Werner state ρ_W, remains in that state for
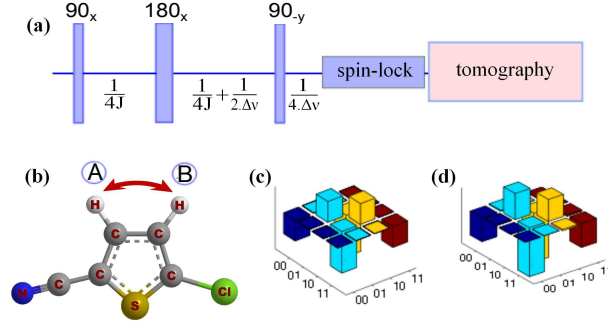
Figure 3.4: The pulse sequence for preparing long-lived singlet states (a), molecular structure of 5-chlorothiophene-2-carbonitrile (b), and traceless real parts of the theoretical (c) and the experimental (d) density matrices. The experimental Werner state in (d) was obtained with a spin-lock of 16.4 s and has a fidelity of 0.99.

several tens of seconds, and ultimately decays towards the uniform state $\mathbb{1}/4$ that is the asymptotic eigenstate of the spin-lock evolution after the decay of all spin correlations.

3.4.1 Results

We monitored fidelity of the experimental state relative to the Werner state at 17 spin-lock durations, $\tau = 2^n$ ms with $n = \{0, 1, \cdots, 16\}$). As shown in Fig. 3.5(a), it starts with a value of 0.85, reaches a maximum of 0.99 after a few seconds, and then decreases. The real parts of the deviation density matrices $\overline{\rho}_W$ and $\overline{\rho}(\tau)$, with τ=16.4 s corresponding to the maximum fidelity 0.99, are compared in Figs. 3.4(c) and 3.4(d).

Although fidelity is a good measure of how close a test density matrix is to the target density matrix, it does not capture the global decay of the purity of the density matrix. To monitor the decay of the purity as well as the closeness of the traceless parts of the density matrices, we define attenuated fidelity,

$$F_a = \frac{\text{Tr}[\overline{\rho}(\tau) \cdot \overline{\rho}_W]}{\sqrt{\text{Tr}[\overline{\rho}(0)^2]\text{Tr}[\overline{\rho}_W^2]}} \ . \tag{3.9}$$

Fig. 3.5(a) also displays attenuated fidelity as a function of the spin-lock duration. We observe that it remains close to its initial value 0.85 until about 1 s, and then drops down. In particular, it starts dropping before the fidelity reaches its maximum value, and is 0.36 at τ=16.4 s.

To understand the evolution of the density matrix during spin-lock, we consider a model consisting of exponential equilibration of the $|T_0\rangle$ state
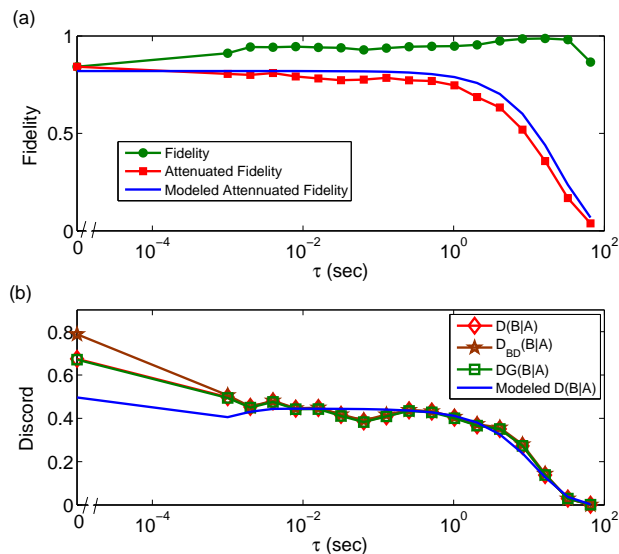
23

Figure 3.5: (a) Fidelity of the experimental state relative to the Werner state as a function of the spin-lock duration τ, and (b) the corresponding values of discord in units of $\epsilon^2/\ln 2$ and geometric discord in units of $\epsilon^2/2$. Discord values were obtained using the methods described in Section II.

with the other triplet states as well as an overall exponential decay of the singlet-triplet mixture towards the uniform identity state:

$$\rho(t) = \frac{1}{4}\mathbb{1} + e^{-\lambda_2 t}\frac{\xi}{4}\Big(\rho_{S0} - e^{-\lambda_1 t}\rho_{T0} - (1 - e^{-\lambda_1 t})\rho_T\Big) \ . \qquad (3.10)$$

Here $\rho_T = \frac{1}{3}\left(|T_1\rangle\langle T_1| + |T_0\rangle\langle T_0| + |T_{-1}\rangle\langle T_{-1}|\right\}$, and λ_1 and λ_2 are the decay constants. By fitting the attenuated fidelity of this model to the experimental attenuated fidelity, as shown in Fig. 3.5(a), we determined $\lambda_1^{-1} = 0.75$ ms and $\lambda_2^{-1} = 26$ s. These values indicate the rapid equilibration of the triplet states and the long-lived nature of the singlet state. It can be noticed that λ_1^{-1} is comparable to the RF period during the spin-lock, and λ_2^{-1} is significantly longer than T_1.

We also measured discord during the spin-lock evolution using the methods described in Section II, and the results are plotted versus the spin-lock duration in Fig. 3.5(b). The results for the extensive measurement method $D(B|A)$ and geometric discord $DG(B|A)$ essentially agree (when scaled by appropriate factors), as expected for accurate methods, and indicate that measurement errors in our experiments are rather small. By looking at angular variation of $J(A:B)$ in the extensive measurement method, at $\tau=16.4$ s when the state is closest to the isotropic Werner state, we estimate that the

24

imperfections in our prepared LLS state give around 3% error to discord values.

The discord $D_{BD}(B|A)$ obtained by assuming that the state is of Bell-diagonal form is an overestimate initially, but becomes almost the same as the other two determinations beyond $\tau{=}1$ ms. That means that artifact off-diagonal coherences are present in our prepared state, but they decay rapidly on a time scale comparable to λ_1^{-1}. The discord value for the two-parameter model of Eq.(3.10) is also shown in Fig. 3.5(b). It is accurate once the state becomes Bell-diagonal, but is unable to model the initial behavior. The reason for the initial discrepancy is that the off-diagonal components missing from Eq.(3.10) alter both $I(A:B)$ and $J(A:B)$. Later evolution and the asymptotic vanishing of discord after long durations of spin-lock is governed by the time scale λ_2^{-1}.

3.5   Discord in three-qubit system

Here we considered three nuclear spins of the same isotope, i.e. *Sample 3* shown in Fig. 3.6(a).Pulse program for the preparation of $|000\rangle$ pseudopure state is shown in Fig. 3.6(c),first block. F_1, F_2, and F_3 represent the three fluorine spins which form the three qubits. The broad and unshaded pulses are π pulses. The flip angle and the phase of the other pulses are mentioned on the top of each of them. Each of the spin selective pulse has been obtained by specially designed strongly modulated pulses having Hilbert-Schmidt fidelity of over 0.99. The pulse program consists of three J evolutions. During the first J evolution period $1/2J_{13}$, the π pulses on F_2 (at $\pi/4$ and $3\pi/4$) refocus J_{23} and J_{12} evolutions, while the π pulses on F_1 and F_3 (at $\tau/2$) retain J_{13}. The additional π pulses on F_1 and F_3 just before the $[\pi/4]_{\overline{y}}$ pulse regain the sign of the spin operator terms inverted by the π pulses on F_1 and F_3 in the middle of $1/2J_{13}$ evolution. Similar argument yields the sequence for the J_{12} and J_{23} evolutions. Now, second block in Fig. 3.6(c) represents the circuit to prepare the $|GHZ\rangle = \frac{1}{\sqrt{2}}(|000\rangle + |111\rangle)$ state. Since the $|GHZ\rangle$ state is a symmetric state we can theoretically predict that the value of discord will be equal irrespective of the bipartite system chosen as shown in Fig. 3.9

Secondly we can prepare $|S_0 0\rangle = \frac{1}{\sqrt{2}}(|001\rangle - |100\rangle)$ state, if after preparing the first $|000\rangle$ pseudopure state we (first block Fig. 3.6(c)) use the pulse sequence shown in Fig. 3.7. Here we can predict that bipartite system of size shown in Fig. 3.9(a),(c) will have equal value of discord , while the type of bipartite system as shown in Fig. 3.9(b) will have zero discord, since it represent a classical state.
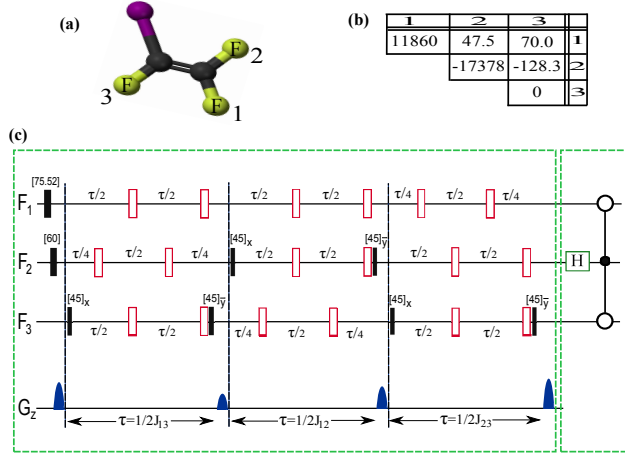
Figure 3.6: (a) The molecular structure of trifloroiodoethylene, and (b) the chemical shifts and scalar couplings.(c)The first block represents the preparation of $|000\rangle$ pseudopure state, and the second block the preparation of GHZ state.
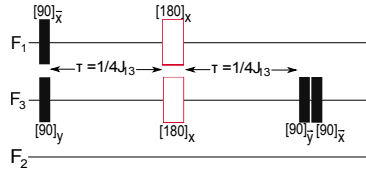

Figure 3.7: Pulse sequence for preparing $|S_00\rangle = \frac{1}{\sqrt{2}}(|001\rangle - |100\rangle)$ state taking $|000\rangle$ as input.
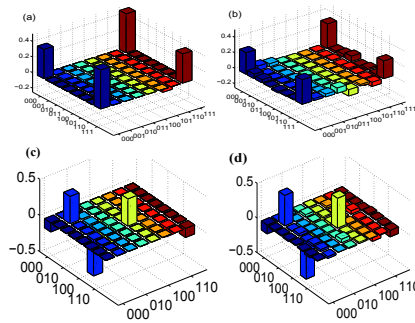

Figure 3.8: Traceless real parts of the theoretical(a),(c) and experimental(b),(d) density matrices of GHZ and $|S_00\rangle$ state respectively. The fidelity of GHZ state is 0.8 and for $|S_00\rangle$ state is .97

26

3.5.1 Results

The state prepared are of the form

$$\frac{1-\zeta/16}{8}\mathbb{1} \quad + \quad \frac{\zeta}{16}(|GHZ\rangle\langle GHZ|) \quad (\epsilon = \zeta/16) \tag{3.11}$$

$$\frac{1-\zeta/16}{8}\mathbb{1} \quad + \quad \frac{\zeta}{16}(|S_00\rangle\langle S_00|) \quad (\epsilon = \zeta/16) \tag{3.12}$$

Values of Discord $DG_{F_1}(\rho_{123})$, $DG_{F_2}(\rho_{123})$, and $DG_{F_3}(\rho_{123})$ are respectively for the $|GHZ\rangle$ mixed state of Eq. (3.11) prepared of fidelity '.80' are '0.4269','0.310', and '0.614' respectively in the units of $\epsilon^2/2$. Here the subscripts denotes the measured qubit. These values as predicted theoretically should have been equal, but due to the low fidelity of the state this kind of anomaly is presented

Discord values $DG_{F_1}(\rho_{123})$, $DG_{F_2}(\rho_{123})$, and $DG_{F_3}(\rho_{123})$ are respectively for the $|S_00\rangle$ mixed state of Eq. (3.12) prepared of fidelity '0.97' are '0.701', '0.014', and '0.702' respectively in the units of $\epsilon^2/2$.
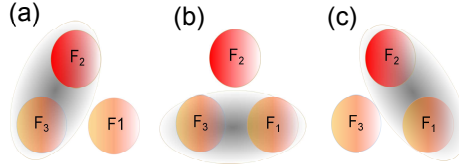

Figure 3.9: Discord is always calculated between the two parts of a system. In case of three qubits we have 3 ways to choose this bipartite division as shown in (a),(b), and (c). Here F_1, F_2, and F_3 represents 1st, 2nd, and 3rd qubit respectively. The unshaded qubit is measured.

Chapter 4

Discussion

Now the main thing is done, I hold certain facts from which I cannot separate. What I know, what is certain, what I cannot deny, what I cannot reject-this is what counts.

– Albert Camus

It is well-known that an ensemble of nuclear spin systems at ordinary NMR conditions does not exhibit entanglement. However, the successful demonstrations of NMR quantum information processing indicate that quantum correlations do exist in such ensembles. In this work, we have studied two measures of such quantum correlations, namely discord and geometric discord. We have revisited the theoretical basis of discord as well as geometric discord, and described how one can obtain these for an experimental density matrix using the Werner state as an example.

The experimental study of discord was carried out in three different systems. In one system, we studied preparation of discord using an entangling pulse sequence, and evolution of discord under dynamical decoupling sequences. Discord did not show much improvement under dynamical decoupling sequences, although there was considerable improvement in fidelity.

In the second system, we used the method of long-lived singlet state to prepare the Werner state. We could describe accompanying evolution of fidelity and discord using a simple relaxation model. In both systems, experimental results matched fairly well with theoretical/simulational expectations.

In the third system, we used the three qubit system to calculate the value of geometric discord taking the example of GHZ type Werner state and $|S_0 \otimes 0\rangle$ type Werner state. The results in this case are not close to

the theoretical values due to the low fidelity of the experimental states. Due to time constraints the experimental accuracy can not be increased, but further experiments will be performed to get a better estimation of quantum correlation in a three-qubit systems.

References

[1] P. W. Shor. Algorithms for quantum computation: discrete logarithms and factoring, *foundations of computer science, 1994 Proceedings*, 124-134 (1994)

[2] A. W. Harrow, Avinatan Hassidim, and Seth Lloyd. Quantum Algorithm for Linear Systems of Equations, *Phys. Rev. Lett.* **103**, 150502 (2009)

[3] Lov K. Grover. A fast quantum mechanical algorithm for database search, *arXiv:quant-ph*/9605043v3

[4] Stephen P. Jordan. Fast Quantum Algorithm for Numerical Gradient Estimation, *Phys. Rev. Lett.* **95**, 050501 (2005)

[5] S. L. Braunstein, C. M. Caves, R. Jozsa, N. Linden, S. Popescu, and R. Schack. Separability of Very Noisy Mixed States and Implications for NMR Quantum Computing, *Phys. Rev. Lett.* **83**, 1054 (1999).

[6] I.S. Oliveira *et al.*, NMR Quantum Information Processing (Elsevier, Amsterdam, 2007).

[7] I.L. Chuang *et al.*. Experimental realization of Shor's quantum factoring algorithm using nuclear magnetic resonance, *Nature* **414**, 883 (2001).

[8] R. Jozsa and N. Linden. On the role of entanglement in quantum-computational speed-up. *Proc. Roy. Soc.* A, 459:2011-2032, (2003).

[9] E. Knill and R. Laflamme. Power of One Bit of Quantum Information, *Phys. Rev. Lett.* **81**, 5672 (1998).

[10] J.S. Bell. On the Einstein Podolsky Rosen Paradox, *Physics* **1**, 195 (1964).

[11] H. Ollivier and W.H. Zurek. Quantum Discord: A Measure of the Quantumness of Correlations, *Phys. Rev. Lett.* **88**, 017901 (2002).

[12] L. Henderson and V. Vedral. Classical, quantum and total correlations, *J. Phys.* A **34**, 6899 (2001).

[13] A. Datta, A. Shaji and C.M. Caves. Quantum Discord and the Power of One Qubit, *Phys. Rev. Lett.* **100**, 050502 (2008).

[14] K. Modi, H. Cable, M. Williamson, and V. Vedral.Quantum Correlations in Mixed-State Metrology, *Phys. Rev. X* **1**, 021022 (2011).

[15] K. Modi *et al.*, Quantum discord and other measures of quantum correlation, e-print arXiv:1112.6238 (2011).

[16] B. Dakic, V. Vedral and C. Brukner. Necessary and Sufficient Condition for Nonzero Quantum Discord, *Phys. Rev. Lett.* **105**, 190502 (2010).

[17] R. Auccaise *et al.*. Experimentally Witnessing the Quantumness of Correlations, *Phys. Rev. Lett.* **107**, 070501 (2011).

[18] G. Passante *et al.*. Experimental detection of nonclassical correlations in mixed-state quantum computation, *Phys. Rev. A* **84**, 044302 (2011).

[19] V. Athalye, S.S. Roy and T.S. Mahesh. Investigation of the Leggett-Garg Inequality for Precessing Nuclear Spins, *Phys. Rev. Lett.* **107**, 130402 (2011).

[20] B. P. Lanyon, M. Barbieri, M. P. Almeida, and A. G. White. Experimental Quantum Computing without Entanglement, *Phys. Rev. Lett.* **101**, 200501 (2008).

[21] D.O. Soares-Pinto *et al.*, Nonclassical correlation in NMR quadrupolar systems, Phys. Rev. A **81**, 062118 (2010).

[22] D. DiVincenzo. The physical implementation of quantum computation. *Fortschr. Phys.*, 48, 771, (2000).

[23] C. H. Bennett and G. Brassard. Quantum cryptography: Public key distribution and coin tossing. *Proceedings of IEEE International Conference on Computers, Systems and Signal Processing, New York*, 175, 1984.

[24] S.P. Barnett. Quantum Information, *Oxford master series in atomic, optical, and laser physics*

[25] A. Datta. A conditon for the nullity of Quantum Discord, *e-print arXiv*:1003.5256 (2010).

[26] D. Girolami and G. Adesso. Quantum discord for general two-qubit states: Analytical progress, *Phys. Rev. A* **83**, 052108 (2011).

[27] Q. Chen *et al.*. Quantum discord for two-qubit X states, *Phys. Rev. A* **84**, 042313 (2011).

[28] S. Luo, Quantum discord for two-qubit states, *Phys. Rev. A* **77**, 042303 (2008).

[29] S Luo and S Fu. Geometric measure for quantum discord, *Phys. Rev. A* **82**, 034302 (2010).

[30] S. Rana and P. Parashar. Tight lower bound in geometric measure of bipartite states, *Phys. Rev. A* **85**, 024102 (2012).

[31] A.S.M. Hassan, B. Lari and P.S. Joag. Tight lower bound to the geometric measure of quantum discord, *Phys. Rev. A*, **85**, 024302 (2012).

[32] A. S. M. Hassan, P. S. Joag. Geometric measure of quantum discord and total quantum correlations in a N-partite quantum state, *arXiv*:1202.0104v1

[33] Nature News. The Power of Discord, *Nature*, **474**, 24-26 (2011)

[34] E.M. Fortunato *et al.*. Design of strongly modulated pulses to implement precise effective Hamiltonians for quantum information processing, *J. Chem. Phys.* **116**, 7599 (2002).

[35] T.S. Mahesh and D. Suter. Quantum information processing using strongly dipolar coupled nuclear spins, *Phys. Rev. A* **74**, 062312 (2006).

[36] D.G. Cory, M.D. Price and T.F. Havel. Nuclear magnetic resonance spectroscopy: An experimentally accessible paradigm of quantum computing, *Physica D* **120**, 82 (1998).

[37] D. Leung *et al.*. Experimental realization of a two-bit phase damping quantum code, *Phys. Rev. A* **60**, 1924 (1999).

[38] H.Y. Carr and E.M. Purcell. Effects of Diffusion on Free Precession in Nuclear Magnetic Resonance Experiments, *Phys. Rev.* **94**, 630 (1954).

[39] xS. Meiboom and D. Gill. Effects of Diffusion on Free Precession in Nuclear Magnetic Resonance Experiments *Rev. Sci. Instr.* **29**, 688 (1958).

[40] L. Viola, E. Knill and S. Lloyd. Dynamical Decoupling of Open Quantum Systems *Phys. Rev. Lett.* **82**, 2417 (1999).

[41] G.S. Uhrig. Keeping a Quantum Bit Alive by Optimized Pulse Sequences *Phys. Rev. Lett.* **98**, 100504 (2007).

[42] S.S. Roy, T.S. Mahesh and G.S. Agarwal. Storing entanglement of nuclear spins via Uhrig dynamical decoupling, *Phys. Rev. A* **83**, 062326 (2011).

[43] M. Carravetta, O.G. Johannessen and M.H. Levitt. Beyond the T1 limit: Singlet nuclear spin states in low magnetic field, *Phys. Rev. Lett.* **92**, 153003 (2004).

[44] M. Carravetta and M. H. Levitt. Long-Lived Nuclear Spin States in High-Field Solution NMR, *J. Am. Chem. Soc.* **126**, 6228 (2004).

[45] S. Cavadini *et al.*. Slow Diffusion by Singlet State NMR Spectroscopy, *J. Am. Chem. Soc.* **127**, 15744 (2005).

[46] G. Pileio, M. Carravetta and M.H. Levitt. Extremely Low-Frequency Spectroscopy in Low-Field Nuclear Magnetic Resonance, *Phys. Rev. Lett.* **103**, 083002 (2009).

[47] A.K. Grant and E. Vinogradov. Long-lived states in solution NMR: Theoretical examples in three- and four-spin systems, *J. Magn. Reson.* **193**, 177 (2008).

[48] W.S. Warren *et al.*. Increasing Hyperpolarized Spin Lifetimes Through True Singlet Eigenstates, *Science* **323**, 1711 (2009).

[49] S.S. Roy and T.S. Mahesh. Initialization of NMR quantum registers using long-lived singlet states, *Phys. Rev. A* **82**, 052302 (2010).

[50] S.S. Roy and T.S. Mahesh. Density Matrix Tomography of Singlet States, *J. Magn. Reson.* **206**, 127 (2010).